ISSN 1063-7745, Crystallography Reports, 2015, Vol. 60, No. 2, pp. 185–188. © Pleiades Publishing, Inc., 2015.
Original Russian Text © K.T. Avetyan, L.V. Levonyan, H.S. Semerjian, M.M. Arakelyan, O.M. Badalyan, 2015, published in Kristallografiya, 2015, Vol. 60, No. 2, pp. 207–211.

DIFFRACTION AND SCATTERING OF IONIZING RADIATIONS

Specific Features of Two Diffraction Schemes for a Widely Divergent X-Ray Beam

K. T. Avetyan, L. V. Levonyan, H. S. Semerjian, M. M. Arakelyan, and O. M. Badalyan

Yerevan State University, Yerevan, 0025 Armenia

e-mail: marakelyan@ysu.am

Received April 28, 2014

Abstract—We investigated the specific features of two diffraction schemes for a widely divergent X-ray beam that use a circular diaphragm 30–50 μm in diameter as a point source of characteristic radiation. In one of the schemes, the diaphragm was set in front of the crystal (the diaphragm–crystal (*d–c*) scheme); in the other, it was installed behind the crystal (the crystal–diaphragm (*c–d*) scheme). It was established that the diffraction image in the *c–d* scheme is a topographic map of the investigated crystal area. In the *d–c* scheme at $L = 2l$ (l and L are the distances between the crystal and the diaphragm and between the photographic plate and the diaphragm, respectively), the branches of hyperbolas formed in this family of planes (*hkl*) by the characteristic K_α and K_β radiations, including higher order reflections, converge into one straight line. It is experimentally demonstrated that this convergence is very sensitive to structural inhomogeneities in the crystal under study.

DOI: 10.1134/S1063774515010022

INTRODUCTION

The diffraction pattern formed by a widely divergent beam (WDB) of characteristic X rays contains much information on the specific features of the crystal structure of an object under study, since many Bragg reflections are simultaneously detected in this case.

Currently, there are two methods of X-ray WDB diffraction. In the Kossel method, a point X-ray source is located on the surface of the investigated object or under it; in the pseudo-Kossel method, the point source is located above the surface of an object studied [1–3]. These methods differ in how characteristic radiation is excited, i.e., forming a point radiation source.

In this study we used two somewhat different schemes of WDB diffraction with a standard radiation source, i.e., an X-ray tube with a linear focal spot [4, 5].

In one scheme an X-ray beam passes through a diaphragm in the form of a funnel aperture (30–50 μm in diameter) in a tantalum plate and falls on a crystal under study. The diaphragm, crystal, and photographic plate are placed in a small chamber rotating around the diaphragm axis during exposure. It is only diffracted radiation that falls on a photographic plate mounted behind the crystal. The primary (nondiffracted) radiation is blocked by a trap, the position of which with respect to the radiation source does not change during chamber rotation [4]. In this configuration, referred to as the diaphragm–crystal (*d–c*) scheme (Fig. 1a), the diaphragm works as a point source. When the diaphragm is installed close to the object studied, in front of it or behind it, the scheme is analogous to the Kossel scheme and the diffraction image does not differ from classical Kossel pattern.

When the diaphragm is spaced by a distance of 2–3 mm or more, the scheme is analogous to the WDB

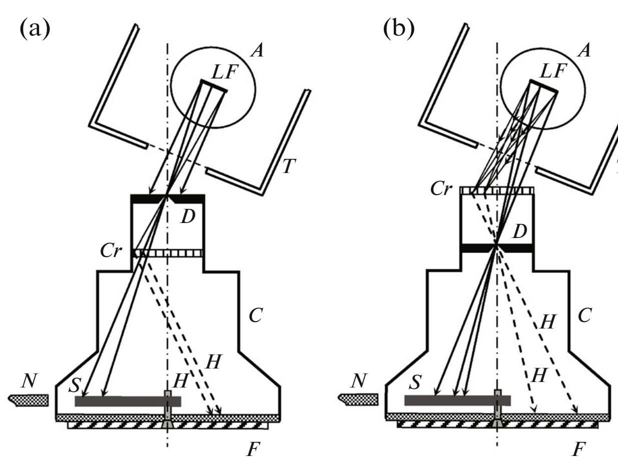

Fig. 1. Schematic diagrams of the experiments in the (a) diaphragm–crystal (*d–c*) and (b) crystal–diaphragm (*c–d*) configurations: (*T*) X-ray tube, (*A*) anode, (*LF*) linear focus, (*C*) chamber, (*Cr*) crystal, (*D*) diaphragm, (*S*) stationary shutter, (*F*) photographic plate, (*N*) permanent magnet, and (*H*) diffracted radiation.

schemes and the diffraction image is a pseudo-Kossel pattern. Thus, a relatively simple scheme allows one to obtain Kossel and pseudo-Kossel patterns of the same sample.

In the other scheme, the crystal studied is exposed to a divergent X-ray beam so as to satisfy the Bragg condition at any point of the crystal area for several sets of atomic planes simultaneously (multiwave diffraction) (Fig. 1b) [5].

The diaphragm is placed at a distance of 2–5 mm behind the crystal. Only the diffracted radiation transmitted through the diaphragm falls on the photographic plate installed behind it. The primary, non-diffracted radiation is trapped. Since the diffraction angle is specified for a certain set of planes (*hkl*) and a given characteristic radiation wavelength, the radiation diffracted at certain points of the crystal can pass through the diaphragm.

We will call these points active and the configuration will be referred to as the crystal–diaphragm (*c–d*) scheme. No analogs of the *c–d* scheme are known.

FEATURES OF THE *c–d* AND *d–c* SCHEMES

In the *c–d* scheme, the distribution of active points on the crystal surface is determined by the following requirement: the radiation diffracted at an active point $M(x_1y_1z_1)$ of the crystal surface passes through the diaphragm. If the origin of the rectangular system of coordinates is aligned with the diaphragm center and the axis *OZ* coincides with the normal to the photographic plate (diaphragm axis), we have the following relation for active points:

$$x_1\cos\alpha + y_1\cos\beta + z_1\cos\gamma = -\sqrt{x_1^2 + y_1^2 + z_1^2}\sin\theta_{khl},$$

where α, β, and γ are the angles between the [*hkl*] direction and the coordinate axes. This is the equation for conical surfaces with axes coinciding with the [*hkl*] directions and a vertex common for all sets of atomic planes (*hkl*) and coinciding with the diaphragm center. The cross sections of the conical surfaces by the $z_1 = l$ plane (outer crystal face) form a set of hyperbolas:

$$\begin{aligned} &x_1^2(\cos^2\alpha - \sin^2\theta) + 2x_1y_1\cos\alpha\cos\beta \\ &+ y_1^2(\cos^2\beta - \sin^2\theta) + 2x_1l\cos\alpha\cos\gamma \\ &+ 2y_1l\cos\gamma + l^2(\cos^2\gamma - \sin^2\theta) = 0. \end{aligned} \quad (1)$$

Thus, active points are distributed over hyperbolas in the *c–d* scheme.

The conical surfaces extend infinitely to both sides from the vertex and intersect with the $z = -L$ plane, where the photographic plate is located. The diffraction image formed on the latter is a set of conical cross sections, i.e., hyperbolas, determined as

$$\begin{aligned} &x^2(\cos^2\alpha - \sin^2\theta) + 2xy\cos\alpha\cos\beta \\ &+ y^2(\cos^2\beta - \sin^2\theta) + 2Lx\cos\alpha\cos\gamma \\ &+ 2Ly\cos\beta\cos\gamma + L^2(\cos^2\gamma - \sin^2\gamma) = 0. \end{aligned} \quad (1a)$$

Since hyperbolas (1) and (1a) are similar (the angular coefficients of asymptotes are the same), the distributions of active points on the crystal surface and the diffraction maximum on the photographic plate are unambiguously consistent; i.e., each active point $M_1(x_1, y_1)$ on the crystal surface corresponds to a single point $M(x, y)$ in the diffraction image. In other words, the diffraction image formed in this scheme is a magnified image, or a topographic map, of the distribution of active points with a magnification factor $K = L/l$.

In the *d–c* scheme, the crystal is exposed to a divergent X-ray beam passing from the diaphragm, which acts as a point source placed behind the crystal. The distribution of active points on the crystal surface is determined by the following condition: the angle Φ_1 between the incident beam, passing through the diaphragm and point $M(x_1, y_1)$ (vector $\mathbf{K}_0$), and the normal to the (*hkl*) plane (vector **H**) is $\pi/2 + \theta$. Consequently, if the investigated crystal in the form of a thin plate is installed in the $z = -l$ plane, the distribution of active points on the crystal surface is determined by Eq. (1).

The radiation diffracted at the $M_1(x_1, y_1, z_1)$ point falls onto the photographic plate. The diffraction of distribution peaks on the photographic plate must satisfy, along with (1), the following condition: the angle Φ between the diffracted beam passing through the $M_1(x_1, y_1, z_1)$ point on the crystal surface and the $M(x, y, z)$ point on the photographic plate (vector **K**) and vector **H** is $\Phi = \frac{\pi}{2} - \theta$. If the photographic plate is located in the $z = -L$ plane, the equation for the distribution of diffraction maxima has the form

$$\begin{aligned} &(x - x_1)^2(\cos^2\alpha - \sin^2\theta) + 2(x - x_1)(y - y_1) \\ &\times\cos\alpha\cos\beta + (y - y_1)^2(\cos^2\beta - \sin^2\theta) \\ &+ (x - x_1)(L - l)\cos\alpha\cos\gamma + 2(y - y_1)(L - l) \\ &\times\cos\beta\cos\gamma + (L - l)^2(\cos^2\gamma - \sin^2\theta) = 0. \end{aligned} \quad (2)$$

Taking into account, along with (1) and (2), the complanarity of vectors $\mathbf{K}_0$, **K**, and **H** (i.e., $\mathbf{K}[\mathbf{K}_0\mathbf{H}] = 0$), we obtain

$$\begin{aligned} &(yl - y_1L)\cos\alpha + (Lx_1 - lx)\cos\beta \\ &+ (xy_1 - x_1y)\cos\gamma = 0. \end{aligned} \quad (3)$$

Thus, in the *d–c* scheme, as in any scheme with a point source located at a distance $z_1 = -l$ above the crystal ($z_1 \neq 0$), the distribution of diffraction maxima on photographic plate, mounted at the distance $z = -L$, is determined by Eqs. (1)–(3). In the general case, the equation specifying the distribution of diffraction maxima is of the fourth order [1]. Conse-

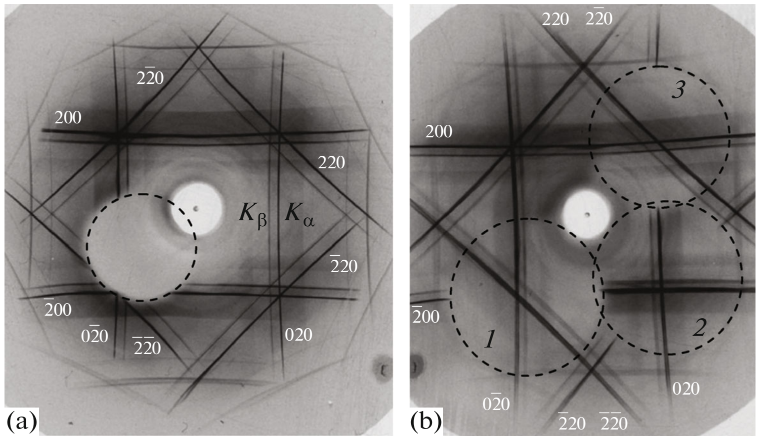

Fig. 2. Diffraction image of LiF crystal obtained within the (a) *c–d* and (b) *d–c* schemes.

quently, in the *d–c* scheme, the diffraction image cannot be similar to the distribution of active points on the crystal surface. Let us consider a simple case where a crystal is oriented so as to satisfy the condition $\cos\alpha = \pm 1$ for the set of (*hk*0) planes. At this orientation, the distribution of active points on the crystal surface is given by

$$x_1^2/l^2\tan^2\theta - y_1^2/l^2 = 1. \quad (4)$$

The distribution of diffraction maxima is determined as

$$x^2/(L-2l)^2\tan^2\theta - y^2/L^2 = 1. \quad (5)$$

Hyperbolas (4) and (5) are not similar because the angular coefficients of asymptotes are different: $y_1 = x_1\cot\theta$ and $y = Lx\cot\theta/(L-2l)$; in the second case, the asymptote angular coefficient depends also on distances L and l. Comparing (4) and (5), one can make sure that the magnification of the diffraction image (the ratio of the coordinates of two hyperbolas) in the real-axis direction (in this case, the *OX* axis is the normal to the plane) differs from that in the imaginary-axis direction (*OY* axis); i.e., we have $k_r = x/x_1 = (2z_1 - z)/z = (2l - L)/l$ and $k_i = y/y_1 = z/z_1 = L/l$ for the real and imaginary axes, respectively.

As the *OX* axis, we can choose the normal to any of the (*hk*0) planes belonging to the *OZ* zone. Consequently, the hyperbolas of the crystal diffraction image that are formed by the characteristic X-ray WDB according to the *d–c* scheme are not similar to the hyperbolas of active points on the crystal surface, like in any scheme with a point source placed in front of the crystal. This means that the diffraction image in the *d–c* scheme is not a topographic map of the crystal.

Let us consider a very important difference between the *c–d* and *d–c* schemes. In the former scheme, any point of the crystal region under study is exposed to X rays in wide angular ranges; therefore, the diffraction is multiwave at all points. The radiation diffracted from a certain plane (*hkl*) is strictly directed. Therefore, when one of the diffracted waves coming from an active point passes through the diaphragm, the other wave coming from the same point cannot pass through it. We may state that the diffraction image is formed by only one diffracted wave in the *c–d* scheme; i.e., each point of the diffraction image receives information from only one corresponding active point. In other words, the diffraction does not exhibit a multiwave character.

Hence, the diffraction image is a topographic map of the active points on the crystal surface in the *c–d* scheme.

In the *d–c* scheme, multiwave diffraction manifests itself in the fact that all diffracted waves, without restriction, reach the photographic plate. In this case the waves diffracted from different active points of the crystal reach a given point in the diffraction image; i.e., the information is superimposed. Therefore, the diffraction image is not a topographic map of the investigated crystal in this case.

EXPERIMENTAL

Figure 2a shows the diffraction image of a LiF crystal, formed by characteristic MoK_α and MoK_β radiations using the *c–d* scheme. The intense lines (hyperbolas) are formed by K_α radiation and the less intense ones are formed by K_β radiation. The white circle at the center is the shadow of a roller containing the primary (nondiffracted) beam trap. The crystal (0.5-mm-thick plate) has a round aperture 0.8 mm in diameter. The larger crystal face, i.e., the (001) plane, is oriented parallel to the photographic plate. The crystal is installed so as to make the aperture image in Fig. 2a be at the intersection point of the hyperbolas formed by the ($\bar{2}00$), ($0\bar{2}0$), and ($\bar{2}\bar{2}0$) reflections (the aperture center is close to the [$\bar{2}\bar{2}0$] site). In the

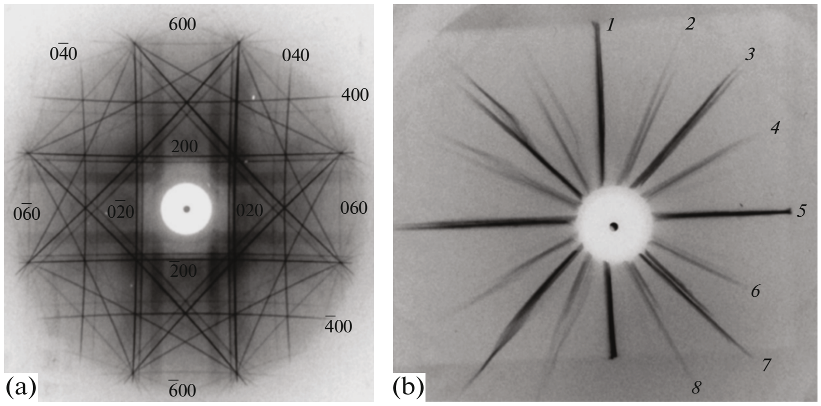

Fig. 3. Diffraction image of KCl crystal obtained within the (a) *c–d* and (b) *d–c* schemes at distances $L = 2l$.

diffraction pattern, one can clearly see the aperture image in the form of a white circle. It can also be seen that the $(\bar{2}00)$, $(0\bar{2}0)$, and $(\bar{2}\bar{2}0)$ hyperbolas are broken at the boundary of the circle image. This means that, in the *c–d* scheme, the circle area in the image contains a signal from only the vicinity of the $[\bar{2}\bar{2}0]$ site, which is limited by the aperture size; signals from the other areas do not arrive at this image point.

Thus, we may state that in the *c–d* scheme there is an unambiguous correspondence between the distribution of active points on the crystal surface and the distribution of the diffraction maximum in the image.

Figure 2b presents a diffraction image of the same LiF crystal, obtained within the *d–c* scheme. The relative positions of the crystal aperture and diaphragm are retained. It can be seen that no clear aperture image is formed in the diffraction pattern. The aperture manifests itself in three different regions in the diffraction pattern. The $(\bar{2}00)$, $(\bar{2}20)$, and (020) hyperbolas are broken, respectively, at the boundaries of regions *1* (the vicinity of the $[\bar{2}\bar{2}0]$ reflection in the pattern), *2* (the vicinity of the $[[\bar{2}20]]$ reflection), and *3* (the vicinity of the [[220]] reflection).

Thus, in the *d–c* scheme, at given positions of the diaphragm and crystal aperture, the radiation diffracted from the region in the crystal bulk containing the aperture passes to the three different regions in the diffraction image and, vice versa, many parts of the diffraction image receive information from different crystal parts. This means that information is superimposed in the *d–c* scheme.

Of special interest is the case $L = 2l$, where the real axis of hyperbolas is $a = (L - 2l)\cot\theta = 0$. In this case, the magnification of the diffraction image in the direction of the real axis (*OX*) is zero, and the hyperbola is transformed into a straight line $x = 0$, which coincides with the *OY* axis. Thus, along with the two branches of each hyperbolas formed in this (*hk*0) plane by the characteristic K_{α_1} and K_{α_2} radiations of all orders, the hyperbolas formed by the K_β radiation also converge into one line. The diffraction image of the KCl crystal obtained within the *c–d* scheme is shown in Fig. 3a.

Figure 3b presents a diffraction image of the same crystal formed within the *d–c* scheme at distances $L = 2l$. One can see that, for some reflections (line *1* in Fig. 3b), along with the two branches of each of the hyperbolas formed by the characteristic K_{α_1} and K_{α_2} radiations of all orders ((020), $(0\bar{2}0)$, (040), $(0\bar{4}0)$, (060), and $(0\bar{6}0)$), the hyperbolas formed by the K_β radiation also converge into one line.

This convergence is observed not for all reflections. Obviously, the complete convergence of the hyperbola branches is possible for crystals of sufficiently high quality, under the condition $L = 2l$. In real crystals, local structural imperfections lead to a situation where different branches of the same hyperbola are differently distorted; as a result one cannot expect the hyperbola branches to converge.

Thus, we can state that the diffraction image obtained under the condition $L = 2l$ can be used to study the structural inhomogeneities of relatively large crystal plates. The efficiency of this technique should be clarified in future detailed investigations.

REFERENCES

1. V. V. Lider, Crystallogr. Rep. **56** (2), 169 (2011).
2. V. Sh. Shekhtman, I. M. Shmyt'ko, L. G. Shabel'nikov, et al., Dokl. Akad. Nauk SSSR, **205**, 4 (1972).
3. V. V. Aristov, V. Sh. Shekhtman, and I. M. Shmyt'ko, Kristallografiya **21** (1), 50 (1976).
4. K. T. Avetyan and M. M. Arakelyan, Kristallografiya **53** (5), 816 (2008).
5. K. T. Avetyan, Crystallogr. Rep. **55** (5), 737 (2010).

Translated by E. Bondareva